A DFT and ^{59}Co Solid-State NMR Study of the Chemical Shielding Property and Electronic Interaction in the Metalloporphyrin System

Xiao-Ping Xu and Steve C. F. Au-Yeung*

Contribution from the Department of Chemistry, The Chinese University of Hong Kong, Shatin, New Territories, Hong Kong

Received April 13, 1999. Revised Manuscript Received February 4, 2000

Abstract: The hybrid density functional theoretical method has been successfully applied to the computation of the ^{59}Co NMR chemical shifts and shift tensor components in a hexacoordinated Co(III) porphyrin system. The calculated results of $[Co(TDCPP)(MeIm)_2]BF_4$ at the B3LYP/6-311G** level using experimental geometry give excellent agreement with the observed values obtained by the solid-state NMR method. Furthermore, the electronic properties of a series of $[Co(TP_xP)(RIm)_2]^+$ (X and R = substituents) systems have been demonstrated to give good correlation with the chemical shielding properties of the central metal as demonstrated by the theoretical calculation. It is proposed that electron-releasing substituents on the porphyrinate ligand transfer electron density to the metal not only via the porphyrin e(π) orbitals but also with the participation of porphyrin nitrogens σ orbitals. Moreover, a number of unresolved issues in the experimental literature concerning the origin of the behavior of the cobalt line widths, axial ligand substitution, and hydrogen bonding have been addressed. An interpretation taking into consideration the influence of the axial ligand orientation on the shielding property of the central metal within the framework of the libration model is proposed. This study demonstrated that the hybrid density functional theoretical method, with its much higher efficiency than that of post-Hartree−Fock methods such as MPn models, will provide a way for understanding the electronic and molecular structures of reasonably large molecules.

Introduction

Considerable attention has been focused on the chemistry of metalloporphyrins because of their unique electronic property that enables them to possess a large variety of chemical and physical properties. Metalloporphyrin compounds have a significant role in the development of optical, electronic, and photophysical materials with improved properties. As well, they are also biologically important compounds responsible for a large variety of synthetic processes involving nucleic acid, proteins, etc.[1,2] Therefore, in-depth knowledge of the structures, electronic interactions, and chemical properties of metalloporphyrins is of great importance toward understanding their relevant chemistry. This aim was actively pursued through the study of the coordination chemistry of the central metal atom in metalloporphyrins. A number of nuclear magnetic resonance (NMR) studies have been reported focusing on the functional dependence of the central metal ion on macrocyclic substitutions, axial ligands variation and the effects of solvents, concentration, magnetic field, temperature, etc.[3−9]

In comparison, there are only limited theoretical investigations of the NMR property related to the central metal atom in metalloporphyrins using empirical[10] as well as quantum chemical[11] methods. The use of the density functional theory (DFT) method as an efficient alternative to the standard post-Hartree−Fock methods such as MPn in ab initio theory for the computation of NMR chemical shifts has been demonstrated independently by Malkin et al.[12] (DFT-IGLO: individual gauge for localized orbitals) and Schreckenbach and Ziegler[13] (GIAO: gauge including atomic orbitals). With the combination of the DFT method and the use of hybrid exchange-correlation (XC) functionals, rapid and accurate calculations targeting the

* To whom correspondence should be addressed. E-mail: scfau-yeung@cuhk.edu.hk.

(1) Lippard, S. J.; Berg, J. M. In *Principles in Bioinorganic Chemistry*; University Science Books: Mill Valley, CA, 1979.

(2) Hettich, R.; Schneider, H.-J. *J. Am. Chem. Soc.* **1997**, *119*, 5638 and references therein.

(3) Geno, M. K.; Halpern, J. *J. Am. Chem. Soc.* **1987**, *109*, 1238.

(4) (a) Hagen, K. I.; Schwab, C. M.; Edwards, J. O.; Sweigart, D. A. *Inorg. Chem.*, **1986**, *25*, 978. (b) Hagen, K. I.; Schwab, C. M.; Edwards, J. O.; Jones, J. G.; Lawler, R. G.; Sweigart, D. A. *J. Am. Chem. Soc.* **1988**, *110*, 7024. (c) Cassidei, L.; Bang, H.; Edwards, J. O.; Lawler, R. G. *J. Phys. Chem.* **1991**, *95*, 7186. (d) Bang, H.; Edwards, J. O.; Kim, J.; Lawler, R. G.; Reynolds, K.; Ryan, W. J.; Sweigart, D. A. *J. Am. Chem. Soc.* **1992**, *114*, 2843. (e) Bang, H.; Cassidei, L.; Danford, H.; Edwards, J. O.; Hagen, K. I.; Krueger, C.; Lachowitz, J.; Schwab, C. M.; Sweigart, D. A.; Zhang, Z. *Magn. Reson. Chem.* **1989**, *27*, 1117.

(5) (a) Baltzer, L.; Landergren, M. *J. Chem. Soc., Chem. Commun.* **1987**, 32. (b) Baltzer, L.; Landergren, M. *J. Am. Chem. Soc.* **1990**, *112*, 2804.

(6) Aldn, R. G.; Ondrias, M. R.; Shelnutt, J. A. *J. Am. Chem. Soc.* **1990**, *112*, 691.

(7) (a) Safo, M. K.; Walker, F. A.; Raitsimring, A. M.; Walters, W. P.; Dolata, D. P.; Debrunner, P. G.; Scheidt, W. R. *J. Am. Chem. Soc.* **1994**, *116*, 7760. (b) Mink, L. M.; Polam, J. R.; Christensen, K. A.; Bruck, M. A.; Walker, F. A. *J. Am. Chem. Soc.* **1995**, *117*, 9329. (c) Mink, L. M.; Christensen, K. A.; Walker, F. A. *J. Am. Chem. Soc.* **1992**, *114*, 6930.

(8) (a) Medek, A.; Frydman, V.; Frydman, L. *J. Phys. Chem.* B **1997**, *101*, 8959. (b) Medek, A.; Frydman, V.; Frydman, L. *Proc. Natl. Acad. Sci. U.S.A.* **1997**, *94*, 14237.

(9) Tavagnacco, C.; Babriele, G.; Costa, G.; Täschler, K.; von Philipsborn, W. *Helv. Chim. Acta* **1990**, *73*, 1469.

(10) Polam, J. R.; Wright, J. L.; Christensen, K. A.; Walker, F. A.; Flint, H.; Winkler, H.; Grodzicki, M.; Trautwein, A. X. *J. Am. Chem. Soc.* **1996**, *118*, 5272.

(11) (a) Godbout, N.; Havlin, R.; Salzmann, R.; Debrunner, P. G.; Oldfield, E. *J. Phys. Chem. A* **1998**, *102*, 2342.

(12) (a) Malkin, V. G.; Malkina, O. L.; Salahub, D. R. *Chem. Phys. Lett.* **1993**, *204*, 80. (b) Malkin, V. G.; Malkina, O. L.; Casida, M. K.; Salahub, D. R. *J. Am. Chem. Soc.* **1994**, *116*, 5898. (c) Malkin, V. G.; Malkina, O. L.; Eriksson, L. A.; Salahub, D. R. In *Theoretical and Computational Chemistry*; Politzer, P., Seminario, J. M., Eds.; Amsterdam, 1995; Vol. 2.

(13) (a) Schreckenbach G.; Ziegler, T. *J. Phys. Chem.* **1995**, *99*, 606. (b) Schreckenbach G.; Ziegler, T. *Int. J. Quantum Chem.* **1996**, 60, 753.

10.1021/ja9911723 CCC: $19.00 © 2000 American Chemical Society
Published on Web 06/22/2000

shielding property of transition metals have been reported.[11,14−17] For example, we have shown that in-depth knowledge of the electronic structure of the central metal and the bonding picture obtained from NMR chemical shielding properties indeed facilitate understanding on issues relating to the photoaquation catalysis reactions in a series of preorganized protonated polyammonium macrocycle cobalticyanide supercomplexes.[15c] More recently, Oldfield et al. evaluated the ^{57}Fe NMR chemical shielding and Mössbauer electric field gradient tensors for a cytochrome *c* model compound, an isopropyl isocyanide, and carbon monoxy-myoglobin model systems, as well as two simple metalloporphyrins containing bis(pyridine) and bis-(trimethylphosphine) ligands using DFT.[11] But no DFT study addressing the correlation of the NMR shielding property of the central metal with the electronic interaction in metalloporphyrins has been reported. In view of the importance of metalloporphyrins, we were stimulated to investigate the NMR shielding properties and their relevance to electronic properties of hexacoordinated Co(III) porphyrins of the type Co(Por)L_2[18] as a probe of the effectivness of the hybrid-DFT method for the study of reasonably large molecules.

Moreover, our interest in hexacoordinated Co(III) porphyrin systems rest with their biological relevance and that they are isoelectronic and structurally similar to Fe(II) hemins, which makes them ideal model systems for the study of reactivity and redox behavior of naturally occurring Fe(II) hemins. Since ^{59}Co NMR is superior to ^{57}Fe NMR because of the exceptionally high sensitivity of the ^{59}Co nucleus, it permits ready experimental measurements of not only the isotropic chemical shifts but also elements of the anisotropic chemical shielding tensor. This unique property enables a very stringent test of the reliability of the theoretical calculations. It is also well-known that cobalt is an important metal in the B_{12} family of nonpolymeric biomolecules; therefore, it is an ideal candidate for NMR spectroscopic investigation in the solid state as Fryman et al.[8b] have demonstrated recently in the study of a series of hexacoordinated Co(III) porphyrins, cobalamins, and their derivatives. On the basis of the results obtained from solid-state ^{59}Co NMR measurements, Fryman et al. concluded that solid-phase ^{59}Co NMR is potentially very useful for probing the structural properties of vitamin B_{12}. They also concluded that cobalamins and their derivatives, rather than cobalt porphyrins, may be better model systems for the vitamin B_{12} complex. This important finding provided the impetus for pursuing an effective DFT solution for this family of larger molecules to augment experimental studies. It is anticipated that insights derived from the ^{59}Co chemical shielding property and its relationship to electronic interaction may be useful for the development of other model compounds for the study of the B_{12} family of complexes.

Methods

1. Material. [Co(TDCPP)(MeIm)$_2$]BF_4,[18] for which the single-crystal structure has been determined,[4d] was purchased from Porphyrin Products, Inc. and used as supplied.

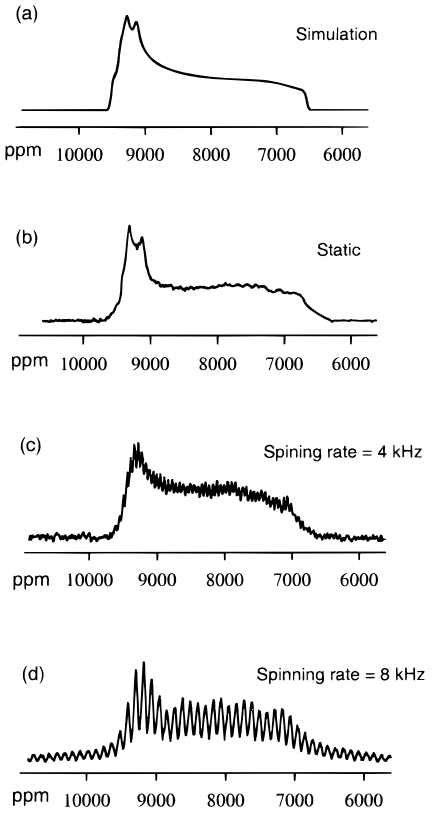

Figure 1. ^{59}Co NMR spectra of [Co(TDCPP)(MeIm)$_2$]BF_4: (a) simulated spectrum with $\delta_{11} = 9430$ ppm, $\delta_{22} = 9210$ ppm, $\delta_{33} = 6600$ ppm, $e^2qQ/h = 13.8$ MHz, $\eta_Q = 0.6$, $\alpha = 0°$, $\beta = 79°$, and $\gamma = 22°$; (b) static spectrum; (c) MAS spectrum with a 4 kHz spinning rate; and (d) MAS spectrum with a 8 kHz spinning rate.

2. Experimental Details. The solid-state spectra of [Co(TDCPP)-(MeIm)$_2$]BF_4 were recorded at room temperature on a Bruker ASX-300 NMR spectrometer operating at 71.2 MHz. A tunable broad-band 5-mm orthogonal Bruker MAS probehead was used to obtain the spectra. An aqueous concentrated K_3[Co(CN)$_6$] solution contained in a 2 mm diameter glass ball was used as an external reference for the determination of the ^{59}Co NMR chemical shifts. Static spectra were collected at different transmitter offsets and coadded into the final powder pattern (Figure 1b) by the spin−echo method to avoid serious spectral distortion due to dead time problem and nonuniform radio frequency excitation power for systems with large anisotropic components. The 16-step phase cycling echo sequence ($\theta-d_1-\theta-d_2-$acquire), suggested by Kunwar et al.,[19] was adopted to eliminate the effects of acoustic ringing. The delay times, d_1 and d_2, were set at 20 and 10 μs, respectively. The relaxation delay was typically set to 0.5 s. The time signal was Fourier transformed on top of the echo after left shifting. Magic angle spinning (MAS) spectra with different spinning rates were measured using the single pulse method in combination with an appropriate phase cycling scheme (Figure 1, parts c and d).

3. Computational Details. The ^{59}Co isotropic chemical shifts and the shift tensor components were calculated using the hybrid DFT-SCF version (using Becke's three-parameter hybrid method and employing the LYP correlation functions, B3LYP)[20] of the GIAO[21] method as implemented in the Gaussian 94 package[22] on a SGI Origin 2000 High-Performance Computing System. A comparison between B3LYP, BLYP (pure DFT), and Hartree−Fock methods was carried

(14) (a) Bühl, M.; Malkin V. G.; Malkina, O. L. *Helv. Chim. Acta* **1996**. *79*, 742. (b) Bühl, M. *J. Phys. Chem. A* **1997**, *101*, 2514. (c) Bühl, M. *Chem. Phys. Lett.* **1997**, *267*, 251. (d) Bühl, M. *Organometallics* **1997**, *16*, 261. (e) Bühl, M. *Angew. Chem., Int. Ed. Engl.* **1998**, *37*, 142.

(15) (a) Chan, J. C. C.; Au-Yeung, S. C. F. *J. Mol. Struct.* (*THEOCHEM*) **1997**, *393*, 93. (b) Chan, J. C. C.; Au-Yeung, S. C. F. *J. Phys. Chem. A* **1997**, *101*, 3638. (c) Zhou, P.; Au-Yeung, Steve, C. F.; Xu, X. P. *J. Am. Chem. Soc.* **1999**, *121*, 1030.

(16) Godbout, N.; Oldfield, E. *J. Am. Chem. Soc.* **1997**, *119*, 8065.

(17) Ruiz-Morales, Y.; Ziegler, T. *J. Phys. Chem. A* **1998**, *102*, 3970.

(18) For the Co(III) porphyrins of the type Co(Por)L_2 studied in this work, Por = tetrakis(2,6-dichlorophenyl) porphyrin (TDCPP), dianion of tetraphenylporphyrin (TP_XP) and porphyrin (POR), and L = RIm with X, R = CN, Cl, H, Me, OMe.

(19) Kunwar, A. C.; Turner, G. L.; Oldfield, E. *J. Magn. Reson.* **1986**, *69*, 124.

(20) (a) Becke, A. D. *J. Chem. Phys.* **1993**, *98*, 5648. (b) Lee, C.; Yang, W.; Parr, R. G. *Phys. Rev. B* **1988**, *37*, 785. (c) Miehlich, B.; Savin, A.; Stoll, H.; Preuss, H. *Chem. Phys. Lett.* **1989**, *157*, 200. (d) Pople, J. A.; Head-Gordon, M.; Fox, D. J.; Raghavachari, K.; Curtiss, L. A. *J. Chem. Phys.* **1989**, *93*, 2537.

(21) Wolinski, K.; Hilton, J. F.; Pulay, P. *J. Am. Chem. Soc.* **1990**, *112*, 8251.

Table 1. Calculated and Experimental ^{59}Co NMR Parameters of $[Co(TDCPP)(MeIm)_2]BF_4$ (values in ppm)

		δ_{11}	δ_{22}	δ_{33}	δ_{iso}
exptl	solid state	9430	9210	6600	8413
	solution				8174[a]
calcd	6-311G**	9190[b]	8977[b]	6293[b]	8153[b]
		9428[c]	9215[c]	6531[c]	8391[c]

[a] From ref 4d. [b] Relative to the absolute shielding of $[Co(CN)_6]^{3-}$ ($\sigma_r = -5400$ ppm).[46] [c] Relative to the shielding intercept ($\sigma_r' = -5162$ ppm).[16]

out. Apart from the all-electron Gaussian basis set 6-311G**, which specifies the 6-311G basis for first-row atoms, the MacLean-Chandler (12s,9p)-(621111,52111) basis sets for second-row atoms,[23,24] and the Wachters-Hay[25,26] all electron basis set for the first transition series, using the scaling factors of Raghavachari and Trucks,[27] augmented by polarization functions,[28,29] and 3-21G*, the locally dense basis sets[30] 6-311G**/3-21G* and 6-311G**/6-31G* were used for addressing their effectiveness. Here 6-311G**/3-21G* denotes a 6-311G** basis for the cobalt and nitrogens and a 3-21G* basis for the other light atoms, and 6-311G**/6-31G* denotes a 6-311G** basis for the cobalt 6-31G* for other light atoms.

Results and Discussion

1. ^{59}Co Chemical Shielding Tensor of $[Co(TDCPP)(MeIm)_2]BF_4$. The experimental ^{59}Co NMR parameters of $[Co(TDCPP)(MeIm)_2]BF_4$ were determined from the static powder spectrum (Figure 1b) by line shape analysis using the iterative SECQUAD program described earlier.[31] The result is presented in Figure 1A and Table 1. The features of the MAS spectra recorded at 4 and 8 kHz spinning rates (Figure 1, parts c and d) essentially approach the shape of the static powder spectrum but in the form of sideband envelopes. Similar spectral features were obtained for the spectrum measured at a spinning rate as high as 12 kHz. This result suggests that the shielding anisotropy is substantial for ^{59}Co in $[Co(TDCPP)(MeIm)_2]BF_4$. Similar solid-state NMR results have been reported for other $[Co(por)(ImMe)_2]$ compounds[8a] with spectra shapes also characteristic of shielding-derived anisotropic patterns. The DFT calculated shielding tensor for $[Co(TDCPP)(MeIm)_2]BF_4$ based on its experimental geometry[4d] is summarized in Table 1. As shown, the calculated shift tensor components ($\delta_{11} = 9428$ ppm; $\delta_{22} = 9215$ ppm; $\delta_{33} = 6531$ ppm) for $[Co(TDCPP)(MeIm)_2]BF_4$ using the hybrid XC-functional DFT method are in excellent agreement with the experimental values ($\delta_{11} = 9430$ ppm; $\delta_{22} = 9210$ ppm; $\delta_{33} = 6600$ ppm) when the value of the intercept shielding determined by Oldfield et al.[16] ($\sigma_r' = -5162$ ppm) is used.

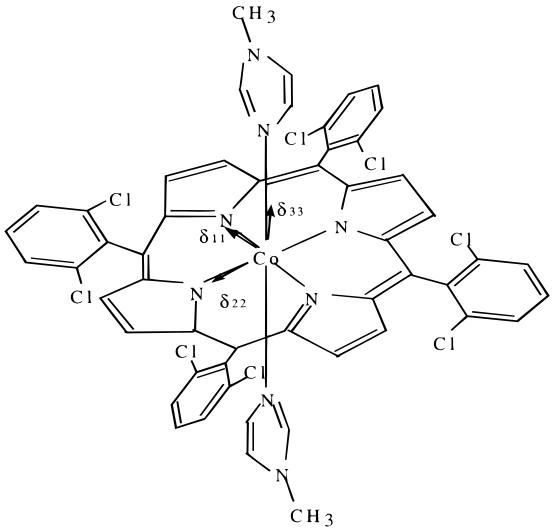

Figure 2. Orientations of the principal components of the ^{59}Co shift tensor for $[Co(TDCPP)(MeIm)_2]BF_4$.

The type of cobalt porphyrin complex discussed herein is close to D_{4h} or C_{4v} symmetry. Such a symmetry is well revealed through the principal axis system (PAS) of the chemical shielding tensor elements of ^{59}Co in $[Co(TDCPP)(MeIm)_2]BF_4$. On the basis of its calculated ^{59}Co eigenvectors, the orientation of the principal components of the chemical shift tensor in the molecular coordinate determined using SYBYL is 7.02° for δ_{11}, 4.72° for δ_{22}, and 1.55° for δ_{33} (Figure 2) for the angles between the tensor components and the metal−ligand bonds. Both the orientations and the values of the chemical shielding tensor elements of the central metal in the PAS for $[Co(TDCPP)(MeIm)_2]BF_4$ confirm that there is a small deviation from ideal D_{4h} (or C_{4v}) symmetry for this complex. This result shows that important information about the PAS chemical shielding tensor, i.e., orientation and magnitudes, which is normally determined by the single-crystal NMR method, may be obtained by a combined powder solid-state NMR and DFT calculation protocol.

Table 2 summarizes the results of a complete evaluation of the effectiveness of the different computation protocol for $[Co(TDCPP)(MeIm)_2]$. The different combinations of computation methods are Hartree−Fock (HF), pure DFT (BLYP), and hybrid DFT (B3LYP) together with the utilization of the basis sets 3-21G, 6-311G**/3-21G*, 6-311G**/6-31G*, and 6-311G**. As shown in Table 2, although the diamagnetic shielding of ^{59}Co converges closely to the free atom value of 2166 ppm calculated by Malli,[32] the agreement between the HF method and experimental results is very poor confirming that the electron correlation effect is significant because the paramagnetic terms of the ^{59}Co chemical shielding are dominant. The data in Table 2 also show that the hybrid-DFT method, B3LYP, is superior to the pure DFT method, BLYP. Both the locally dense basis sets, 6-311G**/3-21G* and 6-311G**/6-31G*, are found to be very effective in the calculation of the cobalt porphyrin system. They give similar results compared with that using the full 6-311G** basis set and requiring much less CPU time. Therefore, the B3LYP/6-311G**/3-21G* locally dense basis set is adopted in the following calculations.

2. Substituent Effects on Shielding and Electronic Property of $[Co(TP_XP)(RIm)_2]^+$ Complexes. Having demonstrated the effectiveness of the hybrid-DFT method for the study of the chemical shielding tensor of the Co(III) porphyrin system using $[Co(TDCPP)(MeIm)_2]BF_4$ as a probe, here we venture to

(22) Frisch, M. J.; Trucks, G. W.; Schlegel, H. B.; Gill, P. M. W.; Johnson, B. G.; Robb, M. A.; Cheeseman, J. R.; Keith, T.; Petersson, G. A.; Montgomery, J. A.; Raghavachari, K.; Al-Laham, M. A.; Zakrzewski, V. G.; Ortiz, J. V.; Foresman, J. B.; Cioslowski, J.; Stefanov, B. B.; Nanayakkara, A.; Challacombe, M.; Peng, C. Y.; Ayala, P. Y.; Chen, W.; Wong, M. W.; Andres, J. L.; Replogle, E. S.; Gomperts, R.; Martin, R. L.; Fox, D. J.; Binkley, J. S.; Defrees, D. J.; Baker, J.; Stewart, J. P.; Head-Gordon, M.; Gonzalez, C.; Pople, J. A. *Gaussian 94, version D.4*; Gaussian, Inc.: Pittsburgh, PA, 1995.

(23) MacLean, A. D.; Chandler, G. S. *J. Chem. Phys.* **1993**, *98*, 5648.

(24) Krishan, R.; Binkley, J. S.; Seeger, R.; Pople, J. A. *J. Chem. Phys.* **1980**, *72*, 650.

(25) Watchers, A. J. H. *J. Chem. Phys.* **1970**, *52*, 1033.

(26) Hay, P. J. *J. Chem. Phys.* **1977**, *66*, 4377.

(27) Ravaghachari, K.; Truks, G. W. *J. Chem. Phys.* **1989**, *91*, 1062.

(28) Clark, T.; Chandrasekhar, J.; Spitznagel, G. W.; Schleyer, P. v. R. *J. Comput. Chem.* **1983**, *4*, 294.

(29) Frisch, M. J.; Pople, J. A.; Binkley, J. S. *J. Chem. Phys.* **1984**, *80*, 3265.

(30) Chesnut, D. B.; Moore, K. D. *J. Comput. Chem.* **1989**, *10*, 648.

(31) Wasylishen, R. E.; Penner, G. H.; Power, W. P.; Curtis, T. D. *J. Phys. Chem.* **1990**, *94*, 591.

(32) Malli, G.; Froese, C. *Int. J. Comput. Chem.* **1967**, *1S*, 95.

Table 2. Comparison of the Calculated Results of $[Co(TDCPP)(MeIm)_2]BF_4$ Using Different Methods and Basis Sets

	method	σ^d (ppm)	σ^p (ppm)	σ_{iso} (ppm)	CSA (ppm)	η	CPU time[a] (h)
HF	3-21G*	2116.3	−54100.5	−51984.1	9941.5	0.298	19.8
	6-311G**/3-21G*	2123.3	−47937.1	−45813.8	7268.3	0.303	22.0
	6-311G**/6-31G*	2159.3	−47532.7	−45373.4	7267.2	0.290	48.9
	6-311G**	2148.1	−47760.9	−45612.7	7294.7	0.302	123.7
BLYP	3-21G*	2131.4	−12551.7	−10420.3	3257.1	0.058	24.8
	6-311G**/3-21G*	2140.6	−11829.2	−9688.6	2671.1	0.068	42.5
	6-311G**/6-31G*	2150.6	−12363.3	−10212.7	2883.5	0.059	78.3
	6-311G**	2164.4	−11947.2	−9782.8	2638.9	0.068	138.7
B3LYP	3-21G*	2128.9	−17136.5	−15007.5	3187.4	0.129	28.1
	6-311G**/3-21G*	2137.1	−15615.3	−13478.1	2806.8	0.115	52.6
	6-311G**/6-31G*	2176.6	−15672.1	−13495.5	2773.1	0.112	83.8
	6-311G**	2160.9	−15714.3	−13553.4	2790.8	0.114	213.2
exptl				−13575[b]	2719.5	0.121	

[a] 4-processor runs on an Origin 2000 High-Performance Computer. [b] Corrected from chemical shift to chemical shielding using the shielding intercept ($\sigma_r' = -5162$ ppm).[16]

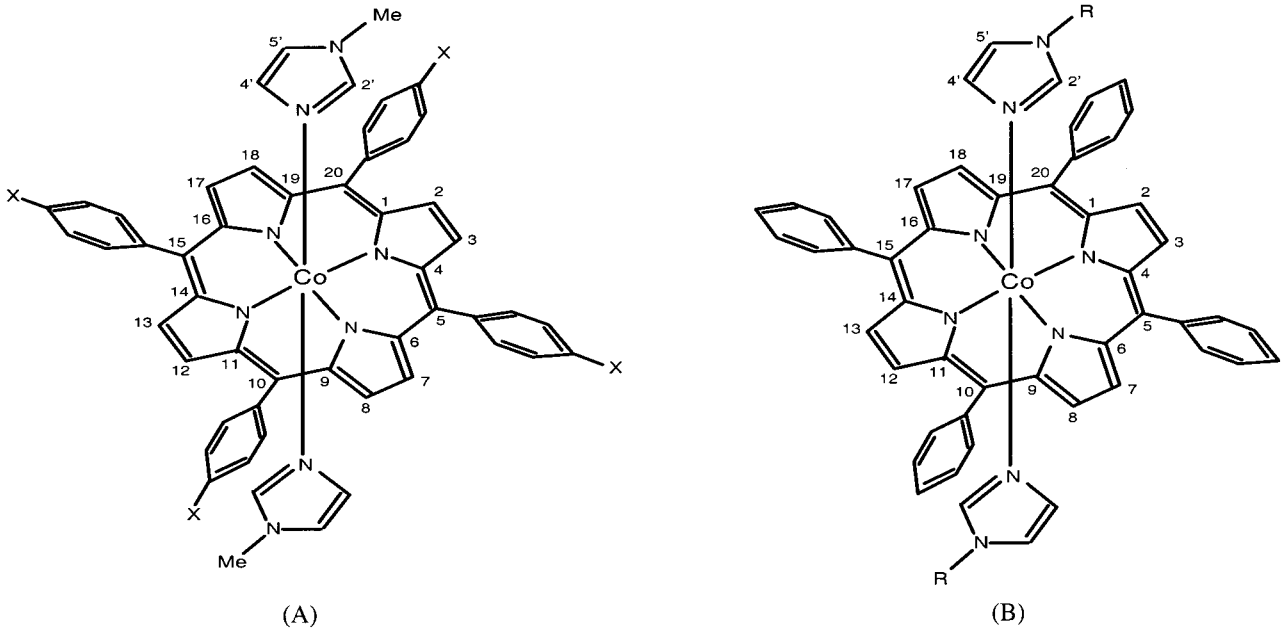

Figure 3. Structural diagram of $[Co(TP_xP)(RIm)_2]^+$ with (A) R = H, X = CN, Cl, H, Me, OMe, and (B) X = H, R = CN, Cl, H, Me, OMe.

apply the method to address the electronic interactions in a series of $[Co(TP_XP)(RIm)_2]$ compounds (Figure 3). In this study, the substituents R and X vary from electron-withdrawing groups, e.g., −CN, −Cl, through −H, to electron-releasing groups such as −Me and −OMe. In the calculations of the chemical shielding of the central metal, the same geometry was adopted for the complex except at positions X or R.

The plot presented in Figure 4A suggests that the cobalt chemical shielding properties correlate with the Hammett constant σ_p for para substituents X (X = OMe, Me, H, Cl, CN) on the phenyl rings of the TP_XP ligand. A correlation is also unveiled for the ^{59}Co chemical shielding properties with σ_m for substituents R on the axial ligand imidazole (Figure 4B). These $\delta_{iso}{}^{59}Co$ versus σ_p trends obtained from theoretical calculations for a series of $[Co(TP_XP)(MeIm)_2]^+$ compounds with different para substituents X on the porphyrin ligand are consistent with those reported in solution NMR studies. The latter was focused on the substitution effects on the isotropic chemical shifts of the central metal in Co(III) and Fe(II) metalloporphyrins.[4b,7b] Note that the trends between the Hammett constants and the isotropic as well as the Hammett constants and the anisotropic shifts are opposite for substituents X and R. The $\delta_{iso}{}^{59}Co$ shifts downfield and the shielding anisotropy increases when X becomes more electron releasing (Figure 4A), but it shifts in the opposite direction when R becomes more electron releasing (Figure 4B). Similar opposing trends were obtained from the theoretical calculation of the parallel component, $\sigma_{||}$, and the perpendicular component, $\sigma_\perp$, of the ^{59}Co chemical shielding versus Hammett constant for X and R (Figure 5).

For $[Co(TDCPP)(MeIm)_2]BF_4$, the single-crystal X-ray study[4d] showed that the axial ligand bond lengths (av. 1.942 Å) are shorter than that of the porphyrin ligand (av. 1.977 Å). On the basis of such a structure, the one-electron d-orbital energy level diagram for d^6 Co(III) in $[Co(Por)(RIm)_2]$ porphyrins with symmetry close to D_{4h} or C_{4v} is arranged as shown in Figure 6.[34] In Figure 6, the lowest energy d−d band splits into two transitions that are of magnitude $\Delta E(^1A_1 \rightarrow {}^1A_2)$ and $\Delta E(^1A_1 \rightarrow {}^1E)$, approximately corresponding to the excitation $d_{xy} \rightarrow d_{x^2-y^2}$ and $d_{xz}d_{yz} \rightarrow d_{z^2}$, respectively. Here the metal−porphyrin bonds are defined as x and y axes; d_{z^2} and $d_{x^2-y^2}$ are σ orbitals on the metal center with d_{z^2} interacting with the axial imidazoles and $d_{x^2-y^2}$ interacting with the porphyrin nitrogens; d_π (d_{xz}, d_{yz}) levels relate to π orbitals on the porphyrin; and the d_{xy} orbital does not interact with the porphyrin or imidazole ligands. Because

(33) (a) Becke, A. D. *J. Chem. Phys.* **1996**, *104*, 1040. (b) Kohn, W.; Becke, A. D.; Parr, R. G. *J. Phys. Chem.* **1996**, *100*, 12974.

(34) Schläfer, H. L.; Gliemann, G. In *Basic Principles of Ligand Field Theory*; John Wiley & Sons Ltd.: New York, 1969; p 51.

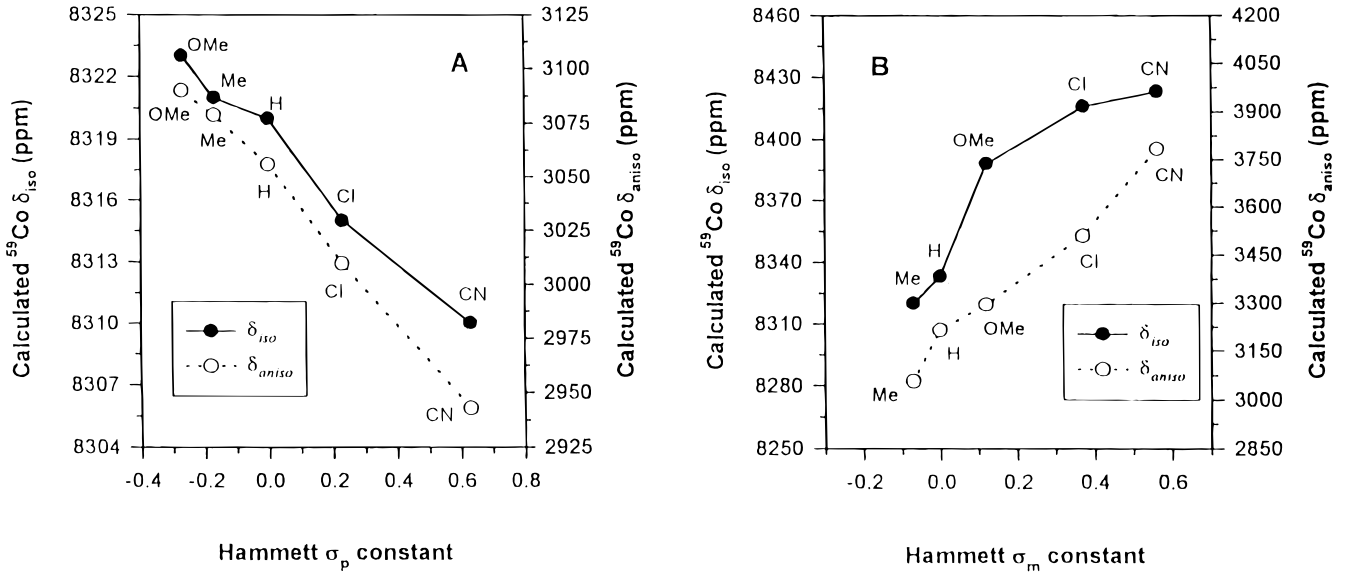

Figure 4. Variation of the ^{59}Co isotropic chemical shifts and chemical shift anisotropies of $[Co(TP_XP)(RIm)_2]^+$ with (A) the Hammett constant, σ_p, for X substituents and (B) the Hammett constant, σ_m, for R substituents.

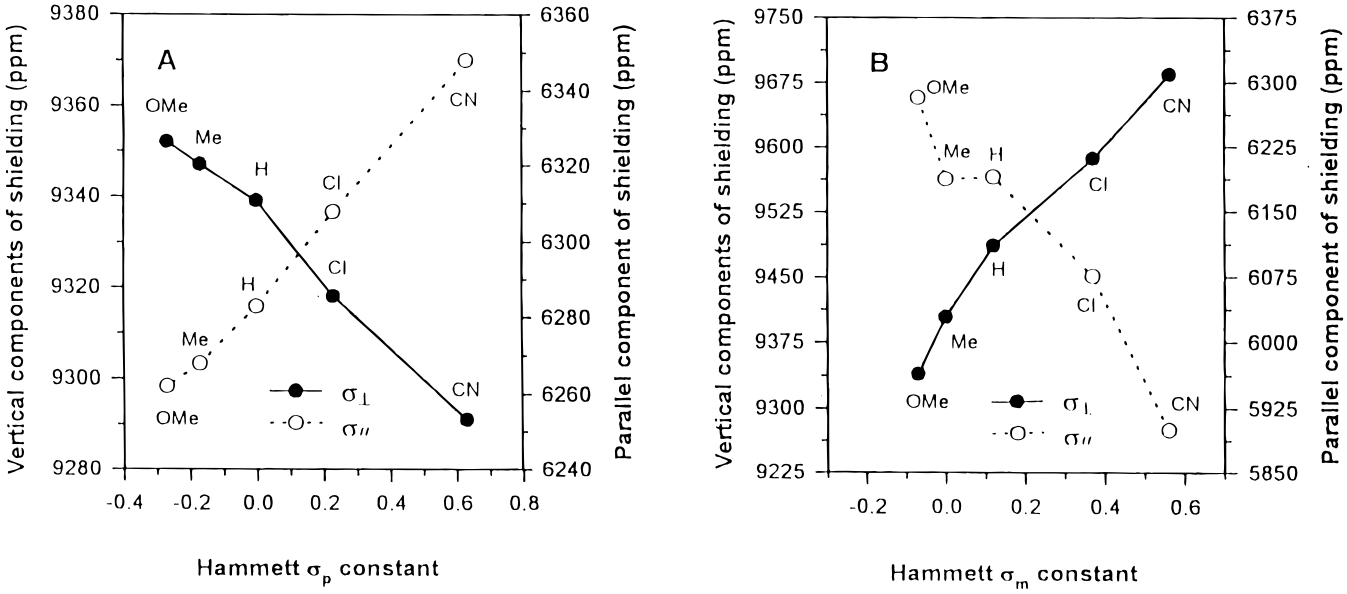

Figure 5. Variation of the^{59}Co chemical shift components of $[Co(TP_XP)(RIm)_2]^+$ with (A) the Hammett constant, σ_p, for X substituents and (B) the Hammett constant, σ_m, for R substituents.

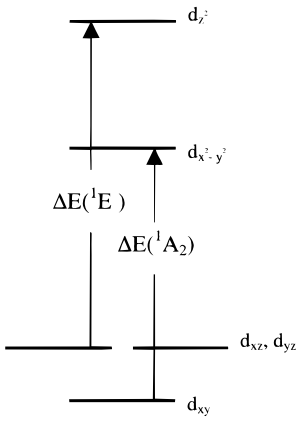

Figure 6. A schematic one-electron d-orbital energy level diagram for the Co(III) porphyrins in this work.

the chemical shifts of octahedral diamagnetic d^6 Co(III) complexes correlate with the ligand field,[35−37] the dominant paramagnetic term of the ^{59}Co chemical shielding for complexes with symmetry close to D_{4h} or C_{4v} can be described as[38]

$$\sigma_{iso}^{para} = -(8\mu_0\mu_B{}^2/\pi)\langle r_d{}^{-3}\rangle\left\{(1/3)\frac{\eta_{\sigma\pi}(^1A_2)}{\Delta E(^1A_2)} + (2/3)\frac{\eta_{\sigma\pi}(^1E)}{\Delta E(^1E)}\right\} \quad (1)$$

where $\langle r_d{}^{-3}\rangle$ is the average value for a single electron in a pure cobalt 3d orbital and η is the covalence factor which has a value close to the nephelauxetic β_{35}. The parallel component $\sigma_{||}$ of the ^{59}Co chemical shielding is related to the transition energy $\Delta E(^1A_2)$ ($d_{xy} \rightarrow d_{x^2-y^2}$) and the perpendicular components $\sigma_\perp$ are connected with the energy $\Delta E(^1E)$ (d_{xz}, $d_{yz} \rightarrow d_{z^2}$, $d_{x^2-y^2}$).

(35) Laszlo, P. In *NMR of Newly Accessible Nuclui*; Laszlo, P., Ed.; Academic Oress: New York, 1983; Vol. 2, p 259.
(36) (a) Freeman, R.; Murry, G. R.; Ricards, R. E. *Proc. R. Soc. London, Ser. A* **1957**, *53*, 601. (b) Griffith, J. S.; Orgel, L. E. *Trans. Faraday Soc.* **1957**, *53*, 601.
(37) Webb, G. A. *Annu. Rep. NMR Spectrosc.* **1991**, 23.
(38) Juranic, N. *Coord. Chem. Rev.* **1989**, *96*, 253.

Therefore, the anisotropic shielding for the complexes considered here is given by

$$\Delta\sigma = \delta_{\perp} - \delta_{\parallel} \approx \sigma_{\parallel}^{\text{para}} - \sigma_{\perp}^{\text{para}} = -8\mu_0{\mu_B}^2/\pi\langle {r_d}^{-3}\rangle\left\{\frac{\eta_{\sigma\pi}(^1A_2)}{\Delta E(^1A_2)} - \frac{\eta_{\sigma\pi}(^1E)}{\Delta E(^1E)}\right\} \quad (2)$$

Using eqs 1 and 2 and the energy level diagram in Figure 6, the trends of the isotropic chemical shift, the shift anisotropy, and the shielding components in relation to the substituent effects in Figures 4 and 5 may be interpreted satisfactorily. That is, for the para substituent acting on the porphyrin, the electron released from the porphyrin ligand to the metal mainly causes a raising in the d_π (d_{xz}, d_{yz}) levels. This effect results in a decrease in $\Delta E(^1E)$ and a concomitant increase in the magnitude of the $\sigma_\perp$ term or in the isotropic chemical shift δ_{iso} as well as an increase in the anisotropic shielding. When the axial substituent, R, becomes more electron releasing, the d_{z^2} level is raised, which leads to an increase in $\Delta E(^1E)$ and hence a decrease in $|\sigma_\perp|$, the isotropic chemical shift and the anisotropic shielding. More importantly, our calculations on shielding components reveal that not only $\sigma_\perp$ but also $\sigma_\parallel$ are influenced in the process of charge transfer. In short, the $d_{x^2-y^2}$ orbital, which interacts with porphyrin nitrogens, also participates in the electron-transfer process. Therefore, for electron-releasing substituents on the porphyrin ligand, the $d_{x^2-y^2}$ level is also raised, thus causing the $|\sigma_\parallel|$ as well as the isotropic chemical shift to decrease and the anisotropic shielding to increase. For electron-releasing substituents on the axial ligand, we suggest that the charge-transfer process toward the metal takes place through the axial ligand, with the porphyrin nitrogen ligand also participating in this process. Thus, the $d_{x^2-y^2}$ level is lowered, which rationalizes the increase in the $|\sigma_\parallel|$ and the isotropic chemical shift but decreases the anisotropic shielding. Since $\sigma_\parallel$ varies in the opposite direction with respect to $\sigma_\perp$, the participation of $\Delta E(^1A_2)$ reduces the substituent effect on the ^{59}Co isotropic chemical shifts but enhances the substituent effect on the ^{59}Co anisotropic shieldings. This is why the latter effect is more significant than the former. Also the results presented in Figure 4 indicate that charge transfer through the axial ligands is more effective than through the porphyrin ligand. Different from conclusions suggested in previous reports,[4a,7b] we concluded that electron transfer to the metal from electron-releasing substituents on the porphyrinate ligand takes place not only via the porphyrin π orbitals but also with the participation of the porphyrin nitrogens σ orbitals. Also, charge density transfer from electron-releasing substituents on the axial ligand to the metal occurs through the σ framework.[39,4e]

3. Controversies: A. Discrepancy between Solid and Solution NMR Results. On the basis of solution ^{59}Co line widths ($\omega_{1/2}$) measurements, it has been concluded[4] that shielding anisotropy is small because $\omega_{1/2}$ has been determined to be independent of the magnetic field strength and that the quadrupolar interaction dominates the relaxation process in Co(III) porphyrin complexes. However, the solid-state ^{59}Co NMR results of [Co(Por)(ImMe)$_2$] compounds[8a] suggested much smaller quadrupolar interaction (~5 MHz) but significant chemical shift anisotropy (~3000 ppm) contributions.

The results of previous studies indicated that different orientations of the axial ligand plane and nonplanar distortion in porphyrins could significantly influence the chemistry of metalloporphyrins and hemoproteins.[40−43] In this study, changes in the orientation of the axial ligand and the nonplanar distortion are considered to be the main conformational changes going from solid to solution. If this is the cause of the discrepancy, a DFT calculation of the ^{59}Co chemical shielding using the model molecule [Co(TPP)(MeIm)$_2$] as a probe may provide insights into this issue. The orientation of the axial ligand plane in metalloporphyrins may be described by the dihedral angle (ϕ) between the axial ligand plane and a second plane defined by a M−N$_p$ bond axis and the axial ligand donor atom (see Figure 7). If the plane defined by an axial ligand plane eclipses a N$_p$−M−N$_p$ bond axis, the value of ϕ is zero and this orientation maximizes bonding interactions.[41a] Minimization of steric interactions between the porphyrin core and the axial ligand occurs at $\phi = 45°$, i.e., the axial ligand plane bisects two N$_p$−M−N$_p$ bond axes. Also, the relative orientation (θ) of the two axial ligand planes may provide additional structural information with the limiting values of θ corresponding to the two axial planes aligning in-plane with each other (parallel, $\theta = 0°$) and perpendicular ($\theta = 90°$) to each other.

Four different combinations of the axial ligand plane orientation were performed and the results are summarized in Table 3. The values in the last column and last row in Table 3 show that the maximum calculated change in shielding anisotropy arising from the effect of axial ligand orientation is 66 ppm. For the nonplane effect, the calculations were first performed

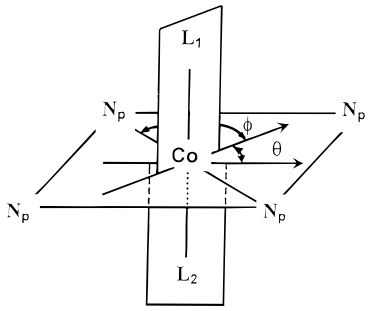

Figure 7. A schematic representation of the orientation of axial ligands in a [Co(Por)L$_2$] type compound.

Table 3. Calculated Orientation Effect of the Axial Ligand Planes on the ^{59}Co Shielding Property of [Co(TPP)(MeIm)$_2$]

	$\theta = 0°$			$\theta = 90°$		
	$\phi = 0°$	$\phi = 45°$	$\lvert\Delta\rvert^a$	$\phi = 0°$	$\phi = 45°$	$\lvert\Delta\rvert^a$
δ_{11} (ppm)	10028	9615	413	9426	9447	21
δ_{22} (ppm)	8691	8981	290	9215	9215	0
δ_{33} (ppm)	6298	6231	67	6291	6236	56
δ_{iso} (ppm)	8339	8276	63	8311	8300	11
δ_{aniso} (ppm)	3061	3066	5	3029	3095	66

[a] $|\Delta| = |\text{data}(\phi = 0°) - \text{data}(\phi = 45°)|$.

(39) (a) Baltzer, L.; Landergren, M. *J. Am. Chem. Commun.* **1987**, *32*. (b) Baltzer, L.; Landergren, M. *J. Am. Chem. Soc.* **1990**, *112*, 2804.

(40) Sparks, L. D.; Medforth, C. J.; Park, M.-S.; Chamberlain, J. R.; Ondrias, M. R.; Senge, M. O.; Simith, K. M.; Shelnutt, J. A. *J. Am. Chem. Soc.* **1993**, *115*, 581.

(41) (a) Scheidt, W. R.; Chipman, D. M. *J. Am. Chem. Soc.* **1986**, *108*, 1163. (b) Scheidt, W. R.; Kirner, J. F.; Hoard, J. L.; Reed, C. A. *J. Am. Chem. Soc.* **1987**, *109*, 1963. (c) Scheidt, W. R.; Lee, Y. J. *Struct. Bonding* (*Berlin*) **1987**, *64*, 1. (d) Walker, F. A.; Huynh, B. H.; Scheidt, W. R.; Osvath, S. R. *J. Am. Chem. Soc.* **1986**, *108*, 5288. (e) Hatano, K.; S. M.; Safo, M. K.; Walker, F. A.; Scheidt, W. R. *Inorg. Chem.* **1991**, *30*, 1643. (f) Safo, M. K.; Gupta, G. P.; Walker, F. A.; Scheidt, W. R. *J. Am. Chem. Soc.* **1991**, *113*, 5497.

(42) Inniss, D.; Soltis, S. M.; Strouse, C. E. *J. Am. Chem. Soc.* **1988**, *110*, 5644.

(43) (a) Gerothanassis, I. P.; Kalodimos, C. G.; Hawkes, G. E.; Haycock, P. *J. Magn. Reson.* **1998**, *131*, 163. (b) Kalodimos, C. G.; Gerothanassis, I. P.; Rose, E.; Hawkes, G. E.; Pierattelli, R. *J. Am. Chem. Soc.* **1999**, *121*, 2903.

Table 4. Calculated Nonplane Effects on the ^{59}Co Shielding Property of [Co(POR)(MeIm)$_2$]

	Co out of the porphyrin plane			ruffling in the porphyrin skeleton		
	flat[a]	Co$_{0.1Å}$[b]	$\|\Delta\|$[d]	flat[a]	ruffling[c]	$\|\Delta\|$[e]
δ_{11} (ppm)	8936	9598	662	8936	9366	430
δ_{22} (ppm)	8792	8542	250	8792	9152	360
δ_{33} (ppm)	6909	7205	296	6909	6396	513
δ_{iso} (ppm)	8213	8449	236	8213	8305	92
δ_{aniso} (ppm)	1955	1865	90	1955	2863	908

[a] [Co(POR)(MeIm)$_2$] with the flat porphyrin plane. [b] [Co(POR)(MeIm)$_2$] with Co 0.1 Å out of the porphyrin plane. [c] [Co(POR)(MeIm)$_2$] with the geometry based on the X-ray structure. [d] $|\Delta|$ = |data(flat) − data(Co$_{0.1\ Å}$)|. [e] $|\Delta|$ = |data(flat) − data(ruffling)|.

on model system Co(POR)(MeIm)$_2$ with (i) a flat porphyrin plane and (ii) the central metal, Co, located out of the porphyrin plane at a 0.1 Å distance. The results presented in Table 4 indicate that the change of shielding anisotropy in Co is about 90 ppm when the central metal deviates from in-plane to out-of-plane at a 0.1 Å distance. When compared with a total span of ∼3000 ppm in the known shielding anisotropy, both the orientation effect of the axial ligands and the out-of-plane effect of the central metal contribute no more than 2−5% change in the shielding anisotropy. It has also been reported that the porphyrin skeleton of [Co(TDCPP)(MeIm)$_2$]BF$_4$ ruffled substantially,[4d] and could be a source modulating the size of the shielding anisotropy. To evaluate its contribution toward shielding anisotropy, chemical shielding was calculated based on the X-ray geometry[4d] of [Co(TDCPP)(MeIm)$_2$]BF$_4$ with all 2,6-dichlorophenyls replaced by protons. The results in Table 4 show that the change in shielding anisotropy, $|\Delta|$, is reasonably significant (∼900 ppm) going from the flat plane to the ruffled plane.

We have also estimated the relative contributions of chemical shielding anisotropy (CSA) and nuclear quadrupolar interaction to the line width $\omega_{1/2}$. Using the ^{59}Co nuclear quadrupolar coupling constant e^2qQ/h(NQCC) = 5 MHz (for most imidazole and *N*-methylimidazole complexes observed in previous studies, NQCC ≈ 3−9 MHz[4,8]) and the asymmetry parameter $\eta = 0$, the contribution from the nuclear quadrupolar interaction is

$$\omega_{1/2} = \frac{3\pi}{10}\frac{2I+3}{I^2(2I-1)}\left(1+\frac{\eta^2}{3}\right)\left(\frac{e^2qQ}{h}\right)^2\tau_c \approx (3.1\times 10^{12})\tau_c \quad (3)$$

whereas the CSA contribution toward the line width in solution at a Larmor frequency ν_L = 71.2 MHz is

$$\omega_{1/2} = \frac{2}{\pi 15}(2\pi\nu_L)^2(\sigma_{||}-\sigma_{\perp})^2\tau_c \approx (7.9\times 10^{10})\tau_c \quad (4)$$

using a CSA value $|\sigma_{||} - \sigma_{\perp}| \sim 3000$ ppm and assuming that the porphyrin plane is flat. Comparing the estimated values, it is readily shown that the contribution to the solution line width resulting from a 3000 ppm shielding anisotropy effect is indeed small, although the contribution to a solid-state NMR spectrum resulting from the same effect dominates when compared with the contribution originating from a NQCC = 5 MHz effect. Using this latter NQCC value and $\tau_c = 1\times 10^{-10}$ s determined for porphyrin complexes in solution,[8a] the calculated line width contribution is 300 Hz which is much smaller than the range of line widths (500−1000 Hz) determined for most porphyrin complexes. In short, the line width contribution resulting from the nuclear quadrupolar interaction in solution is also too small to account for the total metal line width. Therefore, we concluded that for the porphyrin systems in question, other operating relaxation mechanism(s) must dominate the central metal line width.

Table 5. Experimental and Calculated Hydrogen Bonding Effect on the ^{59}Co Shielding Property of [Co(TPP)(HIm)$_2$]

exptl[a]			calcd		
MeOH (mL)	δ_{iso} (ppm)	$\omega_{1/2}$ (Hz)	HB length (Å)	δ_{iso} (ppm)	δ_{aniso} (ppm)
0.00	8384	900	∞	8333	3217
0.03	8379	720	3.05	8297	2906
0.06	8372	700	3.00	8295	2891
0.09	8367	590	2.95	8292	2878
0.15	8363	580	2.90	8290	2859
0.20	8360	650	2.85	8287	2842
0.30	8356	650			

[a] Total volume of solvent (CH_2Cl_2) and MeOH is 3.00 mL.[4b]

B. Discrepancy in Effects of Hydrogen Bonding and Imidazole Substituents on Line Width. Some time ago, Edwards[4b] demonstrated that hydrogen bonds play an active role in determining the cobalt chemical shift in a CH_2Cl_2 solution of [Co(TPP)(HIm)$_2$] (Table 4). When MeOH was added incrementally, the isotropic ^{59}Co chemical shift and line width $\omega_{1/2}$ change significantly in [Co(TPP)(HIm)$_2$]. A subsequent study[4c] further revealed that the NMR line width variations are inconsistent with effects originating from either the formation of hydrogen bonding involving the imidazole in [Co(TPP)(HIm)$_2$] or replacement by bulky but electron rich alkyl groups on the imidazole in [Co(TPP)(RIm)$_2$] (R = methyl, ethyl, *n*-butyl), despite the fact that changes in their chemistry would have enhance the electron-donating power of the axial ligands. While the hydrogen-bonding effect brings about a drop by a factor exceeding 2 in $\omega_{1/2}$, changes in the alkyl group going from methy to ethyl and on to *n*-butyl cause an initial increase in $\omega_{1/2}$ followed by decreases. Moreover, the energy model proposed by Edwards et al. fails to predict the quadrupolar coupling constant as well as $\omega_{1/2}$ in these systems. Using the same energy model, the predictions were successful in the study of substituent effects in [Co(TP$_X$P)(RIm)$_2$] compounds where R and X vary from −CN, −Cl, −H, −Me, and −OMe. That is, with more electron-releasing groups, an increase of the quadrupolar coupling and thus $\omega_{1/2}$ is expected. Attempts to coherently rationalize these observations by invoking changes in τ_c also failed because alkyl substitution or hydrogen bonding should increase the size of the complex, lengthening τ_c and broadening the resonance lines.

A DFT calculation taking into consideration hydrogen bonding involving water molecules with the model complex [Co(TPP)(HIm)$_2$] was carried out. The water molecules were placed at different distances from the coordinated imidazole N−H. The results presented in Table 5 confirm the experimental trend between the chemical shift and the effects of hydrogen bonds on the axial imidazoles.[4a,b] That is, formation of hydrogen bonds causes an upfield shift in the ^{59}Co isotropic chemical shift and a decrease in the ^{59}Co shielding anisotropy. When hydrogen bonding becomes more extensive, both the isotropic shift and the shielding anisotropy decrease. However, the changes in the magnitude of the shielding anisotropy remain too small to fully account for the notable decrease in the observed cobalt line width.

C. Interpretations Based on DFT Calculations and the Libration Model. Cassidei et al.[4c] reported that the solution NMR T_1 values for the axial MeIm in [Co(TPP)(MeIm)$_2$]BF$_4$ compound are significantly longer than the T_1 value of the molecule but appreciably smaller than "free rotation". Other NMR studies[44] also showed that the rotation in Co(III) por-

phyrins with imidazole ligands is slow. Subsequently, a libration model (hindered free rotation about the colbalt-to-nitrogen-3′ bond) has been tentatively proposed by Cassidei et al.[4c] to account for the relaxation behavior observed in $[Co(TPP)(MeIm)_2]BF_4$. We suggest that the origin responsible for the line widths, the axial ligand substitution effect, and hydrogen-bonding effect may be coherently interpreted within the framework of the libration model. According to the DFT results reported in Table 3 (fourth row in the last column), the calculated minimum changes, $|\Delta|$, in the ^{59}Co isotropic chemical shift for ϕ going from $\phi = 0°$ to 45° could be as much as 11 ppm. This difference corresponds to a change of 656 Hz in a magnetic field strength of 5.872 T (^{59}Co Larmor frequency of 59.297 MHz). When compared with the typically observed line width of 1 kHz[4c,d] for cobalt porphyrin complexes, this value amounts to a greater than 50% contribution to the total line width. However, it is expected that an increase in the libration rate or a decrease in the libration amplitude of the axial ligands may reduce such a contribution. In short, there is a significant influence on the line widths when the axial ligand orientation varies as a result of libration motion. Adding this contribution to the line width arising from the nuclear quadrupolar interaction, we arrived at a value (960 Hz) consistent with experimental findings.

Now we turn to the issue involving hydrogen bonding. When the alkyl substituent on axial ligand changes from Me to Et, the libration motion is slowed therefore the line width increases. For cases where the substituent becomes sterically bulky, the rotation motion of the ligand becomes increasingly more difficult. That is, for the subsitituent *n*-C_4H_9, the libration motion would cease or be nearly stopped and thus a drop in line width is observed. Incomplete "cessation" of the libration motion is a possible reason accounting for the fact that the drop in the line width is not as significant as anticipated when R is replaced by *n*-C_4H_9 because measurements were carried out at a higher experimental temperature for R = (*n*-C_4H_9)Im (27.3 °C) compared to that of R = (*n*-CH_3)Im (23.3 °C).

For cases involving hydrogen bonding, bridging of porphyrin complexes or porphyrins and solvent molecules may take place via hydrogen bonding on the imidazole,[45] therefore the libration motion is expected to stop completely and a significant drop in line width appears. Note that the line width decrease (column 3, Table 5) is not directly caused by more extensive formation of hydrogen bonds as suggested,[4b] because a small increase in methanol concentration would not result in enhancement in hydrogen-bonding intensity. Alternatively, increases in the fraction of molecules forming hydrogen bonds in the ensemble would raise the contributions of the hydrogen-bonded species (narrower line width) to the total line width, thereby resulting in a net reduction in the total observed line width.

Conclusions

The present study demonstrates that ab initio quantum chemical calculation at the hybrid DFT level can be successfully implemented for the calculation of ^{59}Co NMR chemical shielding properties in hexacoordinated Co(III) porphyrin systems. The chemical shielding properties of the central metal, as revealed through the isotropic chemical shifts and the shielding anisotropy, give good correlations with the electronic properties of the metalloporphyrins. More importantly, it has been demonstrated that electron-releasing substituents on the porphyrinate ligand transfer electron density to the metal not only via the porphyrin π orbitals but also with the participation of porphyrin nitrogens σ orbitals. Also, DFT calculation results confirm that axial ligand orientation has a significant influence on the shielding property of the central metal. Such an understanding, coupled with the axial ligand libration model, provides a pathway for a coherent interpretation of unresolved experimental issues concerning line widths and axial ligand substitution, as well as hydrogen bonding. It is suggested that the hybrid DFT method could be a powerful tool for obtaining insights into the structure and electronic properties of metalloporphyrins.

Acknowledgment. This research is supported by the Earmarked Research Grant CUHK468/95P from the Research Grants Council of the Hong Kong SAR Government. We would also like to thank the Research Grants Council Central Allocation Scheme (1992) for a grant supporting the purchase of the ASX-300 NMR spectrometer. Support from the Computer Services Center of The Chinese University of Hong Kong on the use of the SGI Origin-2000 High-performance Computing System is gratefully acknowledged. Partial financial support by a Chinese University of Hong Kong One Time Support Grant (1996−1998) is also acknowledged. We thank Dr. Jerry C. C. Chan for helpful discussion.

JA9911723

(44) (a) Polam, J. R.; Shokhireva, T. K.; Raffii, K.; Simonis, U.; Walker, F. A. *Inorg. Chim. Acta* **1997**, *263*, 109. (b) Shokhireva, N. V.; Shokhireva, T. K.; Polam, J. R.; Watson, C. T.; Raffii, K.; Simonis, U.; Walker, F. *J. Phys. Chem. A* **1997**, *101*, 2778.

(45) Lauher, J. W.; Ibers, J. A. *J. Am. Chem. Soc.* **1974**, *96*, 4447.

(46) Bramley, R.; Brorson, M.; Sargeson, A. M.; Schäffer, C. E. *J. Am. Chem. Soc.* **1985**, *107*, 2780.